Construction and Building Materials 427 (2024) 136269

Contents lists available at ScienceDirect

Construction and Building Materials

journal homepage: www.elsevier.com/locate/conbuildmat

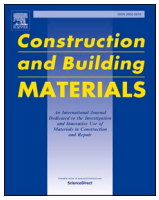

Hydrothermal zeolitization: Towards a paradigm shift for producing stronger and more sustainable construction materials

José Manuel Moreno-Maroto [a,*], Jacinto Alonso-Azcárate [b]

[a] Department of Geology and Geochemistry, Faculty of Sciences, Autonomous University of Madrid, Cantoblanco, Madrid 28049, Spain
[b] University of Castilla-La Mancha. Department of Physical Chemistry, Faculty of Environmental Sciences and Biochemistry, Avenida Carlos III, s/n, Toledo 45071, Spain

ARTICLE INFO

Keywords:
Hydrothermal treatment
Zeolitic construction materials
Zeolite
Geopolymer
Ceramics
Sustainable materials

ABSTRACT

The construction sector provides 14.8 million jobs in the European Union. However, it also accounts for 36% of greenhouse gas emissions and 35% of total waste. High-temperature ceramic manufacturing consumes substantial energy, yielding basic structural products. The alternatives presented, such as geopolymers, still do not replace traditional materials and are not as sustainable as believed. This innovative study combines hydrothermal zeolitization with kaolin-based ceramics fired at both conventional (900°C) and much lower temperatures (600°C), exploring varied conditions, including the use of microplastic wastes as pore-forming agents. Significant zeolite crystallization (15–74%) and mechanical strength increase (2–37-fold compared to untreated materials) is demonstrated in granular specimens, especially when adding microplastics. Geopolymerization appears as a secondary process during treatment. This innovative method offers energy-efficient lower temperatures, transforming fired specimens into zeolite-enriched, robust materials, adaptable to current technology. This study paves the way for further research, opening up a new field of study on hydrothermally manufactured *Zeolitic Construction Materials*.

1. Introduction

Advanced materials are designed to provide technological responses superior to those of their conventional counterparts [1]. Sustainable advanced materials (SAMs) are those whose design, manufacture and performance also represent significant improvements from an environmental, economic and social perspective [2,3]. In a global framework, the European Union (EU) is a world leader in advanced materials, representing 20% of its industrial base. As underlined in the Materials 2030 Manifesto [4], the EU must invest in the development of new SAMs to remain competitive and meet the needs of its citizens. This will require the so-called green and digital transition, harmonized by the European Green Deal [5] and the European Digital Strategy [6], respectively.

Among the nine Materials Innovation Markets included in the Materials 2030 Roadmap is the Materials for Sustainable Construction Market, given the importance of the construction sector at a socio-economic and environmental level [7]. The construction sector is one of the largest employers, with 14.8 million jobs and a turnover of 101.1 billion € in the EU (9% of Gross Domestic Product). This sector is home to 3.3 million companies, of which 2.7 million are small and medium-sized enterprises [7,8]. However, the construction sector is also responsible for approximately 50% of extracted raw materials, 30% of water consumption, 35% of waste generated in the EU, 40% of energy consumption and 36% of greenhouse gas emissions, making it essential to research new SAMs to help alleviate these impacts [7,9].

Although it has traditionally been assumed that the highest energy consumption and negative impacts in the construction sector are linked to the cement and steel industries, the ceramic sector, and specifically brick production, could be placed in comparable figures [10]. This suggests the need to look for alternatives in ceramic production in order to improve manufacturing processes. In addition, the products obtained should exhibit improved properties, thus conforming to the objectives of the Advanced Materials Initiative 2030 [4,7].

Alternative methods of manufacturing construction materials at low temperature have been proposed, highlighting alkaline activation, and more specifically, geopolymerization from raw materials rich in aluminosilicates [11,12]. However, these materials have not yet found a niche that can replace traditional cements and ceramics. In addition, their sustainability can be questioned in many cases, since the activators required for their manufacture are subject to a considerable energy cost (e.g., sodium silicate is produced at 1200–1400°C [13,14]). Also, the control of the rheology in the starting geomaterial dough is a challenge

* Corresponding author.
E-mail addresses: josemanuel.moreno@uam.es (J.M. Moreno-Maroto), jacinto.alonso@uclm.es (J. Alonso-Azcárate).

https://doi.org/10.1016/j.conbuildmat.2024.136269
Received 11 February 2024; Received in revised form 25 March 2024; Accepted 12 April 2024
Available online 16 April 2024

to be considered, generally requiring the use of molds in the manufacture. This is not very feasible when the shape is intended to be given by, for example, extrusion, something very common in the ceramic sector.

In this study, a novel method for manufacturing construction materials based on the alkaline hydrothermal treatment of macroscopic specimens is proposed. Kaolin and polyethylene (PE) and rubber (RB) microplastics have been used as raw materials. The four main objectives have been: (i) to perform the manufacturing process at significantly lower temperatures than traditional ceramic sector standards; (ii) to easily control the rheology, allowing adaptation to processes like ceramic extrusion; (iii) equal or even exceed the mechanical performance compared to only sintered materials; and (iv) to achieve zeolite enrichment through hydrothermal treatment. The latter would lead to the development of a new advanced material with added value compared to traditional construction materials. Previous investigations have demonstrated the adsorbent and decontaminating capacities in geopolymer-zeolite composites [15] and zeolitized brick powder [16,17]. However, it is worth noting that zeolitization has not been carried out in fired macroscopic specimens in any of the mentioned cases. Therefore, the findings of this research could represent a more adaptable and sustainable methodology for the constructive ceramics industry.

2. Materials and methods

2.1. Raw materials

Three raw materials were used: kaolin clay and two microplastics, one powdered polyethylene (PE) and one powdered rubber (RB). The kaolin was supplied by Caobar, S.A. (Taracena, Spain). Its particle size parameters according to laser diffraction results (Coulter® LSTM 230 equipment) are: mean particle size = 8.3 μm; d10 = 0.3 μm; d50 = 4.6 μm; d90 = 18.2 μm. This kaolin is free of organic and inorganic carbon according to TOC-analyzer (Shimadzu® TOC-VCSH). Its X-Ray Fluorescence (Thermo ARL ADVANT'XP Sequential XRF) chemical composition from major to minor oxides is: SiO_2 = 50.9%; Al_2O_3 = 35%; Fe, K and S oxides= 0.4% each; Ca, Mg, Ti and P oxides = 0.1% each. The mineralogy of kaolin according to quantitative determination by X-Ray Diffraction (XRD) with Rietveld refinement (see test conditions in Section 2.3) is: kaolinite = 84.9%; illite = 2.5%; quartz = 2.6%.

Regarding the microplastics investigated, these were artificially prepared. In the case of PE, this is a medium-density PE-hexene linear copolymer. The material was milled at low temperature with a Cumberland® 3050 mill. Its particle size distribution by sieving reveals the following values: mean particle size = 0.334 mm; d10 = 0.056 mm; d50 = 0.338 mm; d90 = 0.482 mm. In the case of the RB powder, it was provided by the company SIGNUS-Valoriza (Chiloeches, Spain) as a product of tire recycling. Its particle size distribution parameters by sieving are: mean particle size = 0.514 mm; d10 = 0.258 mm; d50 = 0.458 mm; d90 = 0.874 mm.

2.2. Manufacture of fired materials and subsequent zeolitization

Three dry starting formulations were prepared: 1) 100 wt% kaolin; 2) a homogeneous mixture of 90 wt% kaolin + 10 wt% PE; and 3) a homogeneous mixture of 90 wt% kaolin + 10 wt% RB. The Atterberg limits were determined: liquid limit (LL) using the Casagrande method and plastic limit (PL) using the thread rolling test, with the plasticity index (PI) calculated by difference [18]. After confirming that the addition of microplastics did not significantly affect plasticity (LL between 40.7 and 42; PL between 25 and 27.4; PI/LL between 0.35 and 0.39), the optimal moisture content (W_{OP}) for subsequent granulation was calculated as $W_{OP} = PL \times 1.234$ [19].

A simplified diagram of the steps followed in the manufacturing process is shown in Fig. 1. Between 250 and 350 g of each dry formulation were blended with its optimal moisture content, namely 31–34% distilled water. After thorough kneading, spheroidal granular specimens with an average diameter of approx. 10.5 ± 0.5 mm (major diagonal of approx. 11 ± 0.5 mm and minor diagonal of approx. 10 ± 0.5 mm) were manually shaped from the wet dough. After oven drying at 105°C for 24 h, the specimens were fired in a Nabertherm® LH 15/14 programmable muffle. As can be seen in Table 1, two firing temperatures were studied: 600°C and 900°C, remaining at the programmed temperature for 2 h, with a previous heating ramp of 300°C/h.

Considering a liquid/solid ratio of L/S = 8.3 ml/g, between 19 and 20 g of the fired specimens were introduced into a steel reactor with a Teflon vessel and covered with 157–166 ml of 1, 3 or 5 M NaOH solution. The reagent used to prepare the alkaline solutions was NaOH in the form of lentil-shaped pellets (PanReac® – AppliChem, pure, pharma grade). Each reactor, duly closed, was placed in an oven at 80°C or 140°C for 24 or 72 h (Table 1). After that, the basic supernatant was removed and the resulting material was repeatedly washed with distilled water until neutral pH, again removing the supernatant. The specimens were finally dried in an oven at 105°C.

2.3. Specimen characterization

The size of the specimens of each formulation was determined after measuring with a caliper the major diagonal and minor diagonal of 15 specimens, calculating the mean and standard deviation of both values.

The crushing strength (S) of the specimens was determined by vertical load to failure on individual specimens using a Nannetti® FM 96 press. Each specimen was diametrically measured with a caliper in its equilibrium position and then placed on the lower plate of the press, so that by vertical displacement the specimen was crushed against the upper plate, recording the breaking load. To ensure soundness in the results, the test was performed on 10 specimens of each formulation, the final result being the average of those obtained according to Eq. (1) [19–22]:

$$S = (2.8 \cdot F_c) / (\pi \cdot d^2) \quad (1)$$

where:

F_c is the failure force, in N.

d is the dimension of the diagonal of the specimen across which the load is applied vertically, in mm.

Based on the EN-1097–6 standard [23], the water absorption after 24 h of immersion (WA_{24}) and the specimen density (ρ) were

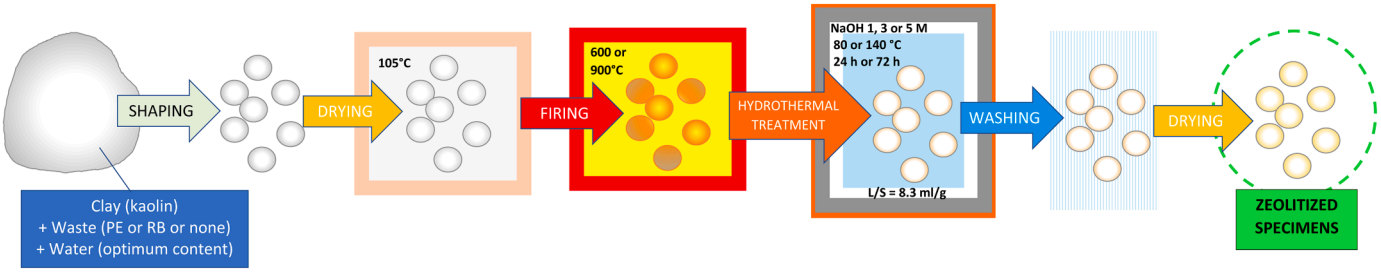

Fig. 1. Simplified flowchart of the steps followed in the manufacturing protocol in this investigation.

Table 1
Formulations of specimens obtained, and firing and hydrothermal treatment conditions applied.

Formulation		Firing		Hydrothermal treatment		
No.	Name	T (°C)	Pore additive	NaOH (mol/L)	t (hours)	T (°C)
1	K900	900	NA	NA	NA	NA
2	K900–3 M(72)-80	900	NA	3	72	80
3	KP900	900	10 wt% PE	NA	NA	NA
4	KP900–3 M (72)-80	900	10 wt% PE	3	72	80
5	KP900–3 M (24)-140	900	10 wt% PE	3	24	140
6	KP900–5 M (24)-140	900	10 wt% PE	5	24	140
7	KR900	900	10 wt% RB	NA	NA	NA
8	KR900–3 M (72)-80	900	10 wt% RB	3	72	80
9	K600	600	NA	NA	NA	NA
10	K600–1 M(24)-80	600	NA	1	24	80
11	K600–3 M(24)-80	600	NA	3	24	80
12	K600–5 M(24)-80	600	NA	5	24	80
13	K600–3 M(72)-80	600	NA	3	72	80
14	KP600	600	10 wt% PE	NA	NA	NA
15	KP600–1 M (24)-80	600	10 wt% PE	1	24	80
16	KP600–3 M (24)-80	600	10 wt% PE	3	24	80
17	KP600–5 M (24)-80	600	10 wt% PE	5	24	80
18	KP600–3 M (72)-80	600	10 wt% PE	3	72	80
19	KR600	600	10 wt% RB	NA	NA	NA
20	KR600–3 M (72)-80	600	10 wt% RB	3	72	80

NA = Not applicable

determined using a water pycnometer as follows:

$$WA_{24} = (M_1 - M_4) / M_4 \cdot 100 \quad (2)$$

$$\rho = \rho_w \cdot M_4 / [M_1 - (M_2 - M_3)] \quad (3)$$

where:

M_1 is the mass of the saturated specimens with dry surface, in g.

M_2 is the mass of the pycnometer containing the saturated specimens after 24 h of immersion in water, in g.

M_3 is the mass of the water filled pycnometer, in g.

M_4 is the mass of the dry specimens, in g.

ρ_w is the density of water at the test temperature (22 ± 3°C), in g/cm^3.

Thus, total porosity (P_T), open porosity (P_O) and closed porosity (P_C) can be calculated as follows:

$$P_T = [1 - (\rho / 2.80)] \cdot 100 \quad (4)$$

$$P_O = \{1 - [(M_4 - (M_2 - M_3)) / (M_1 - (M_2 - M_3))]\} \cdot 100 \quad (5)$$

$$P_C = P_T - P_O \quad (6)$$

where:

2.80 represents the average helium pycnometer density (2.80 ± 0.03 g/cm^3 after testing 5 varieties in triplicate) that the solid phase of the specimens presents after grinding them below 53 μm in agate mortar, determined with an AccuPyc™ 1330 equipment.

The mineralogy of the kaolin and the specimens has been quantitatively determined by X-ray diffraction with Rietveld refinement on randomly oriented powder samples [24,25]. For this purpose, a representative fraction of the specimens was previously ground below 53 μm in an agate mortar. The equipment and conditions used were: PANalytical® diffractometer X'Pert Pro model; 45 kV, 40 mA, CuKα radiation and a system of slits (soller – mask– divergence – antiscatter) of 0.04 rad – 10 mm – 1/8° – 1/2°, with a X'celerator detector and Bragg-Brentano HD module. For the determination of the amorphous phase content, the samples were mixed with ∼ 25 wt% SRM 676a reference alumina. The percentages of each phase were computed by the PANalytical® X'Pert HighScore Plus software.

The changes in chemical bonds during the hydrothermal treatment were studied by Fourier Transform Infrared Spectrometry (FTIR) in nine representative samples ground <53 μm. The equipment used was a Perkin Elmer Spectrum Two™ spectrometer, applying the attenuated total reflectance (ATR) technique. The specific test conditions were: spectral range of 4000–450 cm^{-1}, resolution of 4 cm^{-1}, 20 scans and an aperture of 8.94 mm. The Brunauer-Emmett-Teller (BET) surface area was also measured on <53 μm ground specimens using a Micromeritics Gemini V Surface Area/Pore Size Analyzer, based on N_2 adsorption–desorption isotherms at 77 K. The microstructure of some selected specimens was observed with a Scanning Electron Microscope (SEM), using a Hitachi S-3000 N equipment.

3. Results and discussion

Table 2 and Table 3 show the results obtained on mineralogical compositions and technological properties, respectively. These results will be explained below, discerning between the different manufacturing conditions. Likewise, the diffractograms of the samples are included in Figure S1 (Supplementary material).

3.1. Initial study with samples fired at 900°C

Firing at 900°C resulted in the formation of 89% amorphous phase from the total destruction of the original kaolinite (84.9%), while illite remained at values around 3% (formulation No. 1 in Fig. 2a and Table 2). Although a slight decrease in quartz content is observed (from 12.6% to 8%), such a difference could be considered within the margin of error of the Rietveld quantification, considering that quartz, beyond the α to β transition at 573°C, is not expected to undergo any alteration when fired at 900°C. The resulting material, in the form of metakaolin aggregates, would therefore be thermally activated to facilitate its reactivity in an alkaline medium [26]. A first hydrothermal treatment for 72 h at 80°C in a 3 M NaOH solution has favored the formation of 22.4% zeolite, mainly zeolite A (21.1%) (see formulation No. 2). This zeolite would have been crystallized mainly from the amorphous phase generated during the firing of the aggregates, so that the contribution of quartz and, especially illite, would be marginal. The incorporation of microplastics of polyethylene (PE) or rubber (RB) in the starting formulations has not led to mineralogical changes after firing at 900°C compared to the sample without them (see formulations No. 1, 3 and 7). However, after applying the same hydrothermal treatment as described above, there was a more pronounced increase in zeolite content, which amounted to 48.7% in the mixture with PE (see No. 4 in Fig. 2a and Table 2), and 32.7% in the one with RB (see No. 8), again especially in the form of zeolite A. Such an increase in the formation of zeolites when adding the microplastics would be linked to the open pores that they leave when decomposing during firing, which allows a better entry and hydrothermal reaction of the alkaline solution inside the specimen.

Regarding mechanical strength (Fig. 3a), the non-hydrothermally treated specimens show crushing strengths of 1.3 ± 0.1 MPa and 1.4 ± 0.2 MPa in K900 and KR900 (see No. 1 and 7), respectively, and only 0.4 ± 0.1 MPa in KP900 (No. 3), where the addition of PE would have negatively affected this property. This decrease in mechanical strength when adding PE is consistent with a previous study [19]. These values are within the usual range for granular ceramics, such as lightweight aggregates [22]. After the aforementioned hydrothermal treatment, the

Table 2
Mineralogical composition of the materials obtained. The unfired kaolin is included for comparison.

Formulation		Mineralogical composition (%)											
No.	Name	Kao	Ill	Q	Zeo A	Sod	Zeo X	Can	Hysod	Zeo P1	Am	Σ Kao+Ill+Q	Σ Zeolite
0	Kaolin (unfired)	84.9	2.5	12.6								100	0
1	K900		3	8							89	11	0
2	K900–3 M(72)-80		2.3	6.5	21.1	0.5	0.8				68.7	8.8	22.4
3	KP900		3.2	8.3							88.5	11.5	0
4	KP900–3 M(72)-80		4.3	6.2	46.3	0.9	1.5				40.7	10.5	48.7
5	KP900–3 M(24)-140		2.7	3.5	45.5			2.8	7.7	3.1	34.7	6.2	59.1
6	KP900–5 M(24)-140			0.5	2.1			45	27		25.4	0.5	74.1
7	KR900		3	8.1							88.9	11.1	0
8	KR900–3 M(72)-80			6.2	31.7		0.6		0.4		61	6.2	32.7
9	K600	1.7	2.8	6.3							89.2	10.8	0
10	K600–1 M(24)-80	2	1.4	5.4							91.1	8.8	0
11	K600–3 M(24)-80		2.1	6.6	19.9	0.3	0.7				70.4	8.7	20.9
12	K600–5 M(24)-80		2	7.1	13.5	1	0.5				75.8	9.1	15
13	K600–3 M(72)-80		2.6	6.5	22.4	0.4	0.2				67.9	9.1	23
14	KP600	1.9	2.1	6.6							89.5	10.6	0
15	KP600–1 M(24)-80		0.5	6.1							93.4	6.6	0
16	KP600–3 M(24)-80		2.1	6	31	0.4	0.9				59.6	8.1	32.3
17	KP600–5 M(24)-80		1.7	5.5	31.5	2.9	0.9				57.4	7.2	35.3
18	KP600–3 M(72)-80		2.3	5.6	35.5	0.2	1				55.4	7.9	36.7
19	KR600		2.1	6.7							91.1	8.8	0
20	KR600–3 M(72)-80		2.4	5.4	34.7	0.5	1				56	7.8	36.2

Kao = Kaolinite; Ill = Illite; Q= Quartz; Zeo A = Zeolite A; Sod = Sodalite; Zeo X = Zeolite X; Can= Cancrinite; Hysod = Hydrosodalite; Zeo P1 =Zeolite P1; Am = Amorphous; Σ Zeolite = Zeo A + Sod + Zeo X + Can + Hysod + Zeo P1

Table 3
Technological properties of the materials obtained.

Formulation		Size (mm)		S (MPa)			Density (g/cm^3)		WA_{24} (%)	Porosity, P (%)				BET surface area (m^2/g)
No.	Name	Mean	St. Dv.	Mean	St. Dv.	Ratio	ρ	% var. ρ		P_T	P_O	P_C	% var. P_T	
1	K900	10.25	0.6	1.30	0.15	1.0	1.48	0.0	26.6	47.2	39.5	7.7	0.0	11.0292
2	K900–3 M(72)-80	10.13	0.6	4.55	0.94	3.5	1.78	20.4	11.8	36.5	21.3	15.2	-22.8	9.2076
3	KP900	10.47	0.4	0.38	0.07	1.0	1.20	0.0	34.6	57.0	41.7	15.3	0.0	11.0426
4	KP900–3 M(72)-80	10.7	0.4	4.42	1.37	11.7	1.66	38.1	7.9	40.6	13.2	27.4	-28.7	5.9026
5	KP900–3 M(24)-140	10.26	0.5	5.97	0.74	15.8	1.64	36.3	9.9	41.4	16.3	25.1	-27.4	5.3394
6	KP900–5 M(24)-140	10.17	0.5	7.09	1.44	18.8	1.67	38.9	10.2	40.3	17.2	23.1	-29.3	5.0823
7	KR900	10.41	0.3	1.35	0.20	1.0	1.29	0.0	30.2	53.9	39.2	14.7	0.0	11.3643
8	KR900–3 M(72)-80	10.38	0.4	3.18	1.08	2.3	1.67	29.6	10.3	40.2	17.3	22.9	-25.4	8.8468
9	K600	10.52	0.6	0.55	0.11	1.0	1.48	0.0	24.7	47.0	36.7	10.3	0.0	11.6214
10	K600–1 M(24)-80	10.63	0.5	2.74	0.40	5.0	1.56	5.4	21.7	44.2	34.1	10.1	-6.1	12.0175
11	K600–3 M(24)-80	10.41	0.5	6.34	1.04	11.5	1.74	17.6	12.5	37.7	21.9	15.8	-19.9	11.9627
12	K600–5 M(24)-80	10.4	0.5	4.35	1.43	7.9	1.77	19.1	12.2	36.9	21.7	15.2	-21.5	11.9383
13	K600–3 M(72)-80	10.74	0.4	6.02	1.36	11.0	1.76	18.5	12.3	37.3	21.6	15.6	-20.8	10.3198
14	KP600	10.32	0.4	0.14	0.03	1.0	1.19	0.0	35.6	57.6	42.5	15.1	0.0	9.7923
15	KP600–1 M(24)-80	10.45	0.6	0.72	0.18	5.3	1.25	4.9	28.5	55.5	35.6	19.9	-3.6	12.0656
16	KP600–3 M(24)-80	10.66	0.7	3.18	0.58	23.5	1.52	28.1	12.9	45.6	19.6	26.0	-20.7	7.5728
17	KP600–5 M(24)-80	10.23	0.4	2.52	0.72	18.6	1.60	34.4	10.9	43.0	17.5	25.5	-25.3	7.0875
18	KP600–3 M(72)-80	10.54	0.4	4.99	0.98	36.8	1.61	35.3	11.2	42.6	18.1	24.5	-26.0	7.3575
19	KR600	10.42	0.5	0.28	0.07	1.0	1.26	0.0	30.5	55.1	38.5	16.6	0.0	12.2634
20	KR600–3 M(72)-80	10.55	0.5	4.54	1.07	16.5	1.66	32.1	11.1	40.6	18.5	22.1	-26.2	5.9782

St. Dv. = standard deviation; Ratio = Hydrothermally treated sample / Non-hydrothermally treated sample (same firing conditions). % var. ρ and % var. PT = percentage of variation in the density and total porosity, respectively, of the hydrothermally treated sample compared to the same without hydrothermal treatment.

results were 4.5 ± 0.9 MPa, 3.2 ± 1.1 MPa and 4.4 ± 1.4 MPa, indicating a respective increase in crushing strength by 2.5-fold, 2.3-fold, and 11.7-fold, respectively (see No. 2, 8 and 4 in Fig. 3a). These results suggest that the addition of microplastics would favor the formation of open pores after firing, through which the alkaline solution can easily penetrate. As a result, more zeolite is formed in the structure, increasing the mechanical strength. These improvements are more noticeable when using PE instead of powdered RB, which could be largely due to the fact that the particle size distribution of the former is finer than that of the latter (mean particle size of 0.334 vs. 0.514 mm and d50 of 0.338 vs. 0.458 mm).

Based on these results, two additional hydrothermal treatments have been carried out with the specimens fired at 900°C containing PE, in this case at 140°C for 24 h in 3 M and 5 M NaOH solutions. The treatment with 3 M NaOH has led to the formation of 59.1% zeolite, specifically zeolite A (45.5%), hydrosodalite (7.7%), zeolite P1 (3.1%) and cancrinite (2.8%) (No. 5 in Fig. 2a and Table 2). When using the 5 M solution (formulation No. 6), the developed zeolite percentage exceeded 74%, primarily originating from the amorphous phase, while also leading to the disappearance of illite remnants and nearly all quartz. In this instance, the highly alkaline hydrothermal conditions favored the crystallization of other zeolite species to a greater extent, such as cancrinite (45%) and hydrosodalite (27%), with zeolite A playing a minor role (2.1%). These mineralogical transformations are supported by FTIR results (Fig. 2b), highlighting the following changes in the absorption bands: the highest intensity band, which is found at 1072 cm^{-1} in the

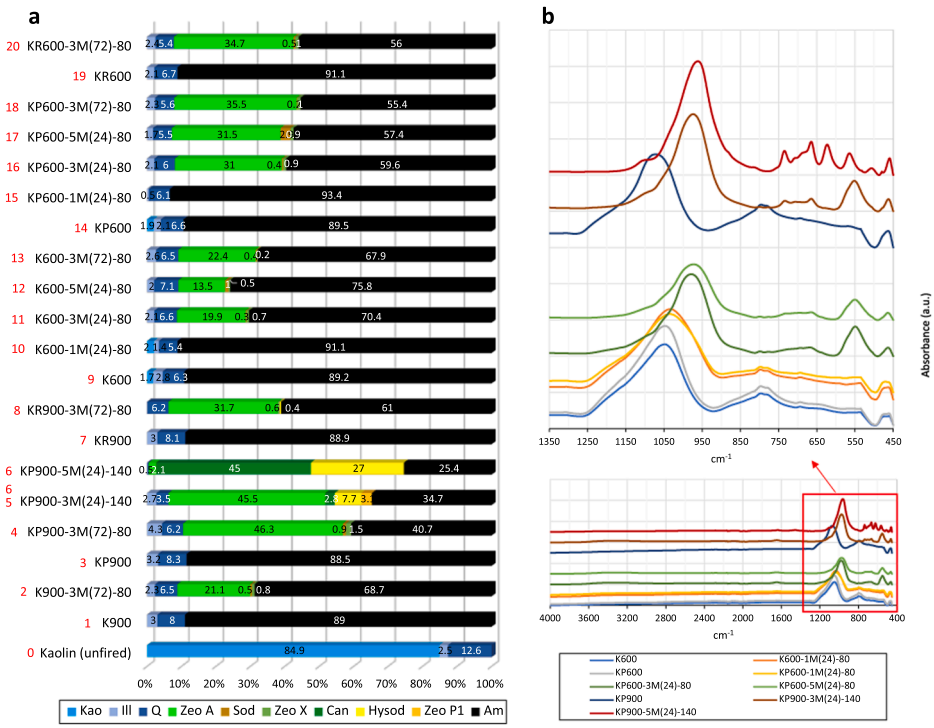

Fig. 2. (a) Mineralogical composition of the materials obtained. The formulation number appears in red next to its name. The unfired kaolin is included for comparison. Kao = Kaolinite; Ill = Illite; Q= Quartz; Zeo A = Zeolite A; Sod = Sodalite; Zeo X = Zeolite X; Can= Cancrinite; Hysod = Hydrosodalite; Zeo P1 =Zeolite P1; Am = Amorphous phase. **(b)** FTIR absorbance spectrum bands from nine representative samples.

sintered-only material, has shifted to 974 cm^{-1} and 961 cm^{-1} after hydrothermal treatment with 3 M and 5 M NaOH, respectively. These bands are linked to asymmetric bending and stretching vibrations in T-O-(T) bonds, where T is Si or Al. The shift towards shorter wavelengths would be linked to a higher participation of Al in the formation of Si-O-Al bonds in the crystallized zeolites [27]. Between 460 and 470 cm^{-1} the peak corresponding to the bending vibrations of the Si-O-Si and Al-O-Al bonds is common in the three samples compared. However, for longer wavelengths, up to approximately 850 cm^{-1}, there is a succession of absorption bands corresponding to symmetric stretching vibrations in T-O-(T) bonds, which in the hydrothermally treated samples differ with respect to the non-hydrothermally treated one. Also, bands have been detected in the zeolitized samples around 3400 cm^{-1}, corresponding to vibrations and stretching of H-O-H bonds and bending of free, pore-adsorbed and surface-adsorbed water molecules in zeolite [28–30]. Concerning the crushing strength, the hydrothermal treatment at 140°C has resulted in 6.0 ± 0.7 MPa when using 3 M NaOH and 7.1 ± 1.4 for the 5 M concentration (Fig. 3a, No. 5 and 6). The increase ratio with respect to the 0.4 ± 0.1 MPa of the untreated sample is 15.8 and 18.8, respectively.

3.2. Hydrothermal treatment of fired samples at 600°C

The tests conducted on specimens fired at 600°C will provide insights into the feasibility of the hydrothermal process in producing hardened materials with significantly lower energy consumption than usual. Those samples not subjected to hydrothermal treatment, simply fired at 600°C from pure kaolin (sample No. 9: K600) and from kaolin mixed with 10 wt% of PE (No. 14: KP600) or RB (No. 19: KR600), exhibit lower mechanical strengths compared to their counterparts prepared at 900°C: 0.5 ± 0.1 MPa vs. 1.3 ± 0.1 MPa, 0.1 ± 0.0 MPa vs. 0.4 ± 0.1 MPa, and 0.3 ± 0.1 MPa vs. 1.4 ± 0.2 MPa, respectively (Fig. 3a). This falls within the expected range, considering that the particle bonding through sintering would be less pronounced. After a 72-hour hydrothermal treatment with 3 M NaOH at 80°C, equivalent to the one initially applied to the specimens fired at 900°C, the crushing strength has increased significantly, surpassing even that of the samples treated at 900°C, reaching 6.0 ± 1.4 MPa in the specimens containing only kaolin (No. 13, Fig. 3a), 5.0 ± 1.0 MPa when adding PE (see No. 18) and 4.5 ± 1.1 MPa with RB (see No. 20). These mechanical strength results far exceed those typical of lightweight aggregates, more closely resembling those of construction ceramics [22]. When compared to the untreated specimens, the mechanical strength has increased by 11 times, 36.8 times, and 16.5 times, respectively, indicating very significant enhancements, especially when PE is added in the form of microplastics. From a mineralogical perspective, the hydrothermal treatment on specimens fired at 600°C has promoted the development of zeolite content ranging from 23% (from pure kaolin samples) to 36–37% (kaolin with PE or RB) (No. 13, 18 and 20 in Fig. 2a and Table 2). These values are similar to those recorded in specimens fired at 900°C, with zeolite A once again standing out as the predominant mineral species. Only in the case of the sample with PE, zeolitization has been lower compared to its counterpart fired at 900°C (36.7% vs 48.7%).

In order to understand the effect of NaOH concentration on the samples fired at 600°C and to further delve into investigating other variables (firing temperature, time, and pore-forming additive), hydrothermal treatments were conducted for 24 h at 80°C using three different NaOH concentrations: 1 M, 3 M, and 5 M. This study has been conducted on kaolin-only specimens (formulations No. 10, 11 and 12 in Table 1) and kaolin specimens fired with PE microplastics (No. 15, 16 and 17, Table 1). Although the addition of PE has involved lower crushing strength results, a similar trend is observed (Fig. 3a). While this property increases in all cases compared to the untreated sample, the lowest values are obtained with the 1 M treatment (2.7 ± 0.4 MPa and 0.7 ± 0.2 MPa), followed by 5 M (4.3 ± 1.4 MPa and 2.5 ± 0.7 MPa), while the intermediate NaOH concentration of 3 M yields the highest strengths (6.3 ± 1.0 MPa and 3.2 ± 0.6 MPa), resulting in maximum enhancements of 11.5-fold and 23.5-fold compared to the untreated samples. This differs, for instance, from the 140°C hydrothermal treatment on specimens fired at 900°C, where higher mechanical strength

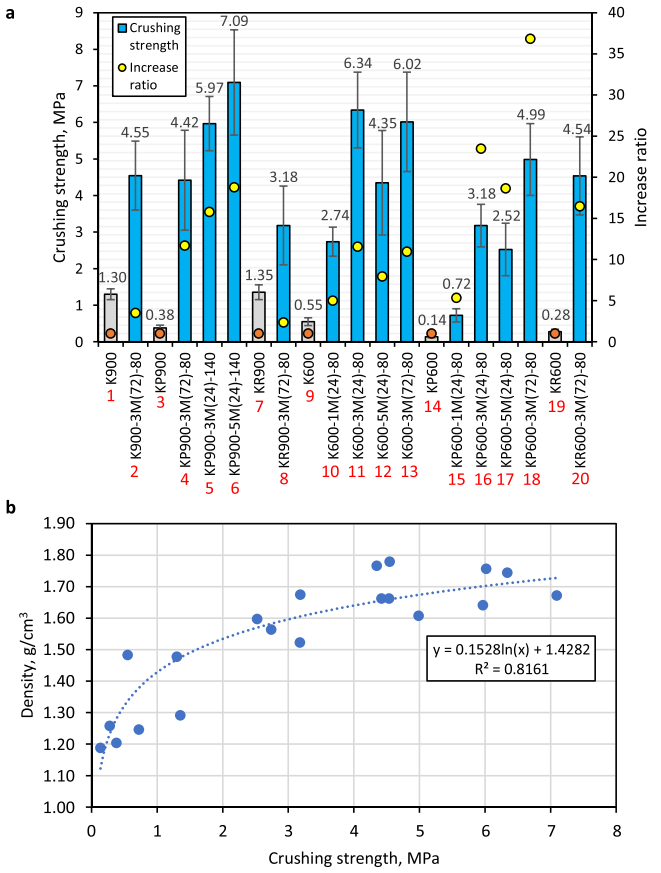

Fig. 3. (a) Crushing strength and increase ratio results obtained for the materials synthetized. The non-hydrothermally treated samples (gray columns with orange circles) are taken as a reference for comparison. The formulation number appears in red under its name. **(b)** Relationship between the density of the samples and their crushing strength.

has been recorded with 5 M NaOH than with 3 M NaOH (see No. 5 and No. 6 in Fig. 3a).

XRD results reveal that the 1 M NaOH solution did not promote zeolite formation, showing minimal differences in the mineralogy of samples with and without PE (see No. 10 and 15 in Fig. 2a and Table 2). Conversely, the 3 M and 5 M concentrations did facilitate zeolite formation (mainly zeolite A), with no significant differences between them. The most distinguishing factor again was the inclusion of microplastics, where zeolite crystallization was much more pronounced: 20.9% vs. 32.3% in the 3 M NaOH solution (No. 11 vs No. 16) and 15% vs. 35.3% in the 5 M solution (No. 12 vs No. 17). Analyzing the FTIR bands (Fig. 2b), the results of the samples fired at 600°C without subsequent hydrothermal treatment are analogous to those explained earlier for the 900°C fired samples rich in zeolite. The same applies to samples treated with 3 M and 5 M solutions when comparing their bands to those of the 900°C fired sample rich in zeolite treated at 140°C with a 3 M solution, thus supporting the XRD findings. However, while no noticeable changes in the band positions are apparent in the samples treated with 1 M NaOH compared to the untreated ones, there is a slight shift of the main band from 1048 to 1033 cm^{-1} and from 1047 to 1035 cm^{-1} in specimens with and without added PE, respectively. The fact that these samples do not contain zeolite suggests the occurrence of a geopolymerization process [28–30], which could also explain the increased mechanical strength in these samples. Therefore, the development of geopolymeric gel could be concurrent with zeolitization in all samples, although the latter would be predominant based on the XRD results obtained.

Regarding the duration of hydrothermal treatment, the results with the 3 M solution for 24 h can be compared to those with the same solution for 72 h, as explained at the beginning of this section. In samples without PE (No. 11 vs No. 13 in Fig. 3a), the crushing strength is similar (6.3 vs 6.0 MPa), while when adding plastic (No. 16 vs No. 18), the 24-hour treatment has been less effective in this regard compared to the 72-hour treatment (3.2 vs 5 MPa). In both cases, the total zeolite formed has only increased slightly with longer treatment time (by 2–4 points; Fig. 2a and Table 2), suggesting that the differences in results may not be solely linked to zeolite formation, once again supporting geopolymerization as another potential involved process.

3.3. *Interrelationship of technological properties*

As demonstrated earlier, the ratio of increase in mechanical strength with hydrothermal treatment has ranged from 2.3 to 36.8, yielding crushing strengths between 2.5 and 7.1 MPa (average of 4.3 ± 1.7 MPa), while the material solely fired yielded values between 0.1 and 1.4 MPa (average of 0.7 ± 0.5 MPa) (Fig. 3a and Table 3). Just as observed in mechanical strength, the density of the specimens has been significantly influenced by the hydrothermal treatment. The firing temperature does not appear to have had a substantial impact on the initial specimens' density, with the incorporation of microplastics playing a more pivotal role. As such, specimens lacking additives exhibit a density of 1.48 g/cm^3 (see No. 1 and 9 in Table 3), while samples containing PE and RB range between 1.19 g/cm^3 and 1.29 g/cm^3 (No. 3, 7, 14 and 19). After application of the hydrothermal treatment, the density has increased, although it is still evident that samples containing microplastics have generally lower densities. For instance, with the 1 M NaOH treatment, the density is 1.56 g/cm^3 (No. 10) vs. 1.25 g/cm^3 for the sample prepared with PE (No. 15). Despite these differences, the increase has been similar in comparison to the untreated specimens, approximately around 5%. For the 3 M and 5 M solutions, in the absence of microplastics, the density varies from 1.74 to 1.78 g/cm^3 (approximately 20% increase over untreated samples), while with PE and RB, the values mainly range from 1.60 to 1.67 g/cm^3 (roughly 30–40% increase), except for the formulation No. 16 (1.52 g/cm^3).

As observed in Fig. 3b, the density increase appears to be a crucial factor in the structural strengthening of the specimens, thus contributing to their improved mechanical strength. This densification process is linked to changes in the porosity of the samples (Table 3). Thus, the 3 M and 5 M NaOH hydrothermal treatments would favor an overall decrease in total porosity of 18–20% in the samples without microplastics and 28–39% in those containing them. This suggests that the zeolitization process is more effective when using the pore-forming additive, since the pores left after firing allow, on the one hand, a better penetration of the alkaline solution along the structure of the fired specimen, and on the other hand, more space available for the zeolite to nucleate and subsequently crystallize. This was not the case when the 1 M NaOH solution was applied, with both resulting samples (No. 10 and 15) showing porosity reductions of approximately 5%, suggesting that the hydrothermal conditions have not been intense enough to produce substantial mineralogical and physical changes even when using PE. However, as indicated in the previous section, the 1 M treatment has shown that geopolymerization could also be involved in mechanical improvements, also linked to a higher densification of the structure.

The type of porosity most affected is the open type, as it is involved in the circulation of the alkaline fluid during the hydrothermal treatment. This aspect is also reflected in a noticeable decrease in the water absorption capacity of the samples, transitioning from values around 30% to close to 10% in a significant portion of the samples (Table 3). SEM microscopy images (Fig. 4) show that the crystallization of zeolites, especially on the surface of these pores, would be responsible for the partial or complete closure of such porosity. Depending on the treatment performed and the developed zeolites, the zeolite crystals exhibit different morphologies, highlighting cubic and 'desert rose' habits in

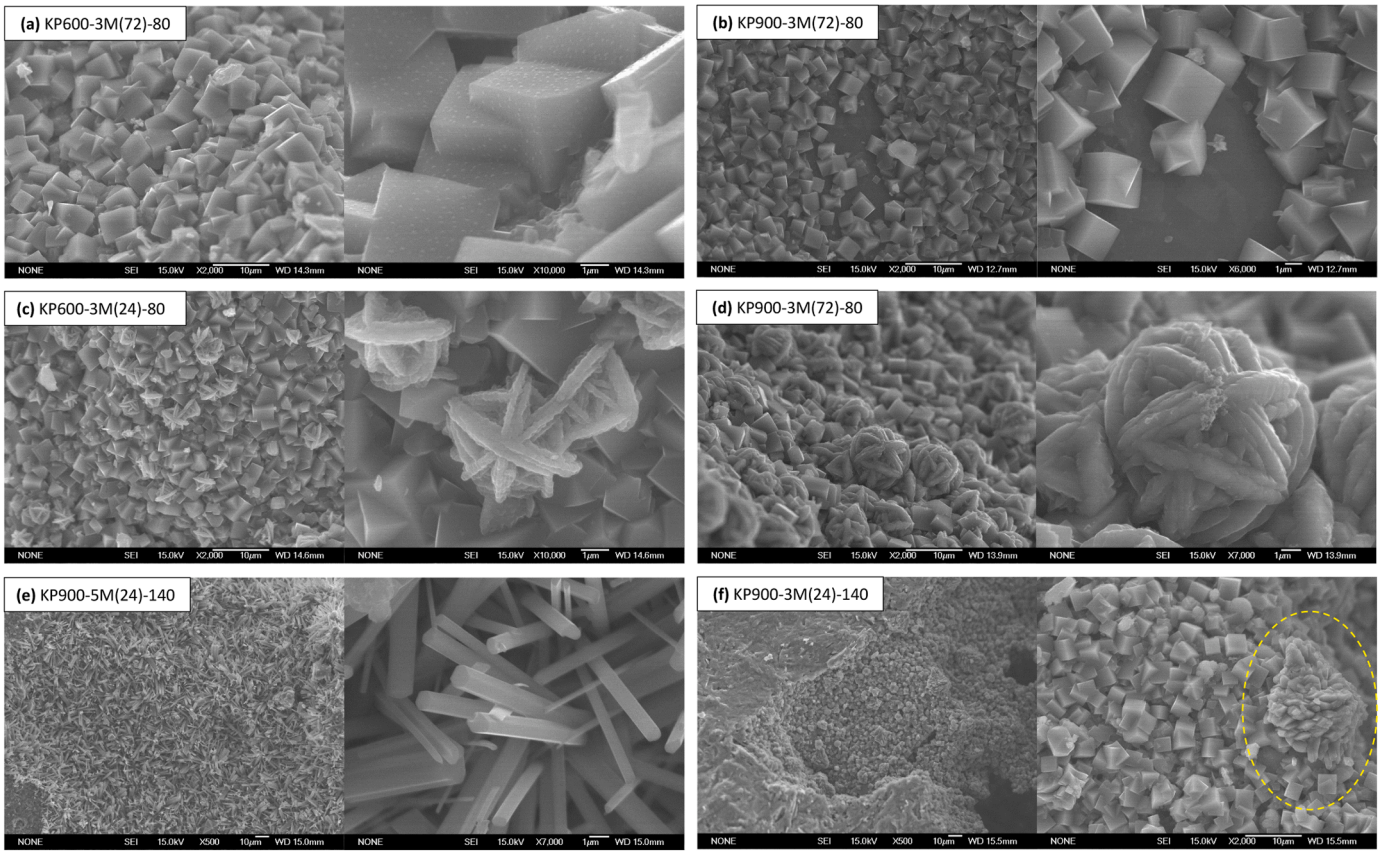

Fig. 4. Details of zeolite crystals taken by SEM microscopy, indicating the sample in each photo: **(a)** and **(b)** cubic habit crystals; **(c)** and **(d)** crystals with desert rose habit between cubic crystals; **(e)** acicular crystals of hexagonal section; **(f)** zone with cubic crystals and crystals with pineapple habit (one of them bordered with yellow line).

samples with a high content of zeolite A (Fig. 4a-d), and acicular habits in the sample rich in cancrinite and hydrosodalite (Fig. 4e). Other crystal habits have also been found, e.g., pineapple (Fig. 4f). The BET surface area results corroborate the reduction of porosity as a consequence of zeolite growth in the pores (Table 2). BET surface area has transitioned from values around 10–12 m^2/g in the non-zeolitized samples to values around 5 m^2/g in those samples with higher zeolite crystallization (Fig. 5).

4. Main findings and future prospects

The results shown in the previous sections show that zeolitization, and geopolymerization to a lesser extent, from fired macroscopic specimens is feasible. Of particular interest is the application of pore-forming agents, such as the microplastics studied, which favor better penetration of the alkaline solution. This leads a more effective zeolitization, densification of the structure and its mechanical strengthening. In the latter case, there is a notable increase ranging from 2-fold to 37-fold compared to the initial crushing strength value.

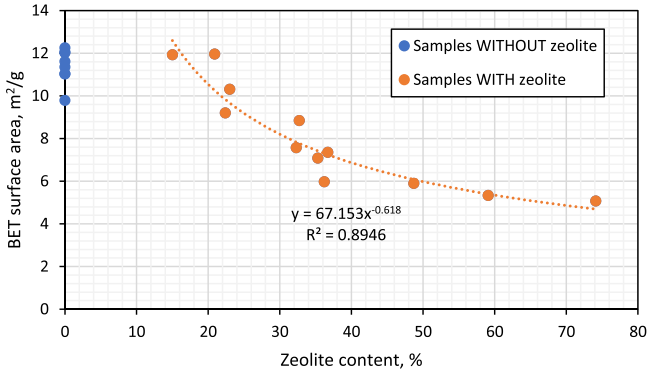

Fig. 5. Relationship between the BET surface area and the crystallized zeolite content in the samples.

Porosity control of the fired specimen, especially open porosity, is a key factor in the subsequent hydrothermal treatment. This is dependent on the type, proportion and size of the pore-forming additive, as well as the firing temperature, since a lower firing temperature leads to a less compact structure. This could be crucial when aiming to develop larger-sized pieces using this method (such as bricks or tiles), as it is necessary to ensure uniform treatment throughout the entire cross-section of the piece. This aspect is especially important, since the specimens used in this research present a spheroidal shape, with an average size of 10.4 ± 0.5 mm, and therefore research with other shapes and sizes could lead to other types of adjustments in the fabrication protocol and mixtures. Despite this, the materials obtained in this work could already have a place in the market as artificial lightweight aggregates, meeting the required minimum density criterion (<2 g/cm^3, [31]). Therefore, the incorporation of pore-forming additives, whether microplastics or others, and less intense firing conditions could be key in this regard. Moreover, it is worth nothing that this study also provides a solution to microplastics, which has a highly negative impact on the environment, not only in aquatic organisms, but also in soil fauna [32]. The other variables studied, including the time and especially the hydrothermal treatment temperature and alkaline concentration, also significantly affect the results.

With regard to geopolymerization, as observed in those hydrothermally treated samples without zeolite formation, it may also be key in

the development of a more compact and stronger structure. Despite this, assuming that the geopolymer gel is amorphous and that the amorphous phase tends to reduce with hydrothermal treatment to form zeolites (Fig. 2a), it can be deduced that geopolymerization would have a secondary role with respect to crystallized zeolites in defining the technological properties of the material obtained.

An important finding in this investigation is that specimens with excellent technological properties (high mechanical strength, low density, and reduced water absorption) can be obtained from a firing stage at a much lower temperature than usual in the ceramic sector, only 600°C compared to the usual over 900°C. This could potentially lead to significant energy and economic savings in such industries, with a concomitant reduction in emissions from combustion. Such reduction in production costs could be reflected in more affordable products in the market.

Furthermore, the improvements observed with the hydrothermal treatment of the specimens were not only notable for low firing temperatures (600°C), but also for temperatures of 900°C, more typical in the ceramics sector. This raises a promising avenue to be studied even in construction ceramics already on the market (commercial bricks, tiles, artificial aggregates, etc.), which could be subjected to hydrothermal treatment and thus examine how their properties are affected. Likewise, these results, together with others reported in hydrothermally treated geopolymers [15] invite to investigate this technique also in other precast elements, such as cements, mortars and concrete.

In addition to this, the process proposed here has other important advantages over currently available technologies. The fact that the material obtained has a high zeolite content could give *decontaminating* capability to the construction materials developed, since the properties of zeolites in this sense are well known [15,33]. Thus, not only would the emissions in their production be lower, but they could help reduce the concentrations of pollutants in the surrounding environment.

Furthermore, other potential research avenues involve exploring the utilization of diverse raw materials apart from the investigated kaolin, including macroscopic pieces from different clay types. This line appears promising, as the successful zeolitization and geopolymerization from various powdered clays are well-documented [15,33]. If favorable outcomes are achieved using raw materials already exploited in the ceramic industry, production could notably benefit from reduced energy consumption, the valorization of strategic wastes (such as microplastics) and the creation of zeolite-rich materials with potential environmental remediation properties. The developed construction materials would thus offer added value compared to the current ones.

From an operational point of view, the manufacturing system proposed here is easily adaptable to the existing industry. By taking advantage of the plasticity and rheology of the clay, prior to firing and subsequent hydrothermal treatment, the pieces can be shaped using any of the techniques already established in the ceramic sector, such as extrusion, pressing, slip casting, hand shaping, 3D printing, etc. This differs from other alternative materials, such as geopolymers, which generally require the use of molds, making their incorporation into processes that require extrusion generally not viable. Additionally, while geopolymers are considered sustainable, their alkaline treatment typically involves the use of activators like sodium silicate, produced at temperatures of 1200–1400°C [13,14]. Despite the extensive academic research on geopolymers, these materials still have minimal presence in the actual market, raising questions about their viability as a real alternative. In contrast, the proposed hydrothermal treatment operates at significantly lower temperatures (e.g., 600°C) and could be easily integrated into existing production lines on the market.

Based on the above, this work opens up a new field of study on *Zeolitic Construction Materials* (e.g. zeolitic bricks, zeolitic aggregates, zeolitic tiles, etc.), potentially more sustainable and advanced than their conventional analogues. The fact that it integrates ceramic, zeolitization and, to a lesser extent, geopolymerization processes opens the possibility of investigating a multitude of variables, such as: different types and proportions of raw materials (giving priority to waste) and reagents, preparation technique of the starting specimens, shape and size of specimens, temperatures and times for firing and hydrothermal treatment, concentration of alkaline solution, liquid-solid ratio, possibility of seeding with previously synthesized zeolites, aging, etc.

5. Conclusions

Based on the above, the main conclusions of this study can be summarized as follows:

- The new hydrothermal treatment proposed, when applied to previously fired kaolin-based ceramic specimens, leads to a significant crystallization of zeolite, which improves the technological properties of the resulting material.
- The zeolite formed facilitates a significant increase in the mechanical strength of the resulting material (2–37-fold), which still has a sufficiently low density to be considered as 'lightweight'.
- The zeolite formed could also provide technological properties superior to those of traditional construction ceramics, such as adsorbent and decontaminating capacity.
- The use of thermally decomposable agents, such as microplastic waste, is promising to promote the formation of pores during firing, which subsequently facilitate better penetration of the alkaline solution, and thus a more effective hydrothermal zeolitization.
- Geopolymerization could act as a secondary process during treatment and could further enhance the mechanical performance to that already provided by zeolite crystal growth.
- The new protocol presented in this study is fully adaptable to existing practices in the ceramic industry, while also enabling operation at significantly lower temperatures than conventional ones in the sector. This results in greater energy efficiency and, consequently, a potential reduction in environmental impact and production costs.
- This study paves the way for further research, for instance by exploring diverse manufacture conditions and raw materials, thus opening up a new field of study on hydrothermally manufactured *Zeolitic Construction Materials*.

CRediT authorship contribution statement

Jacinto Alonso-Azcárate: Writing – review & editing, Investigation. **José Manuel Moreno-Maroto:** Writing – review & editing, Writing – original draft, Visualization, Resources, Project administration, Methodology, Investigation, Funding acquisition, Conceptualization.

Declaration of Competing Interest

The authors declare that they have no known competing financial interests or personal relationships that could have appeared to influence the work reported in this paper.

Data availability

Data will be made available on request.

Acknowledgments

This research was conducted as a part the project "Aplicación de residuos plásticos marinos como componentes tecnológicos en la fabricación de cerámicas zeolitizadas (OZEONIC)" framed within the 6th Edition of the Premios Mares Circulares (Circular Seas Awards) in its Research Projects 2023 modality, funded by Asociación Chelonia and promoted by Coca-Cola Europacific Partners. Special thanks to the companies SIGNUS and Valoriza for providing the rubber waste.

Appendix A. Supporting information

Supplementary data associated with this article can be found in the online version at doi:10.1016/j.conbuildmat.2024.136269.

References

[1] E. Valsami-Jones, F.R. Cassee, A. Falk, From small to clever: What does the future hold for the safety and sustainability of advanced materials? Nano Today 42 (2022) (2022) 101364 https://doi.org/10.1016/j.nantod.2021.101364.

[2] U. Berardi, Clarifying the new interpretations of the concept of sustainable building, Sustain. Cities Soc. 8 (2013) 72–78, https://doi.org/10.1016/j.scs.2013.01.008.

[3] P. Samani, A. Mendes, V. Leal, J. Miranda Guedes, N. Correia, A sustainability assessment of advanced materials for novel housing, Build. Environ. 92 (2015) 182–191, https://doi.org/10.1016/j.buildenv.2015.04.012.

[4] AMI2030, Materials 2030 Manifesto: Systemic Approach of Advanced Materials for Prosperity – A 2030 Perspective, Adv. Mater. Initiat. 2030. 7 Febr. 2022. (2022). ⟨https://www.ami2030.eu/wp-content/uploads/2022/06/advanced-materials-2030-manifesto-Published-on-7-Feb-2022.pdf⟩.

[5] European Commission, 2019. Communication from the Commission to the European Parliament, the European Council, the Council, the European Economic and Social Committee and the Committee of the Regions. The European Green Deal. COM(2019) 640 final. Brussels, 11.12.2019. https://eur-lex.europa.eu/resource.html?uri=cellar:b828d165-1c22-11ea-8c1f-01aa75ed71a1.0002.02/DOC_1&format=PDF.

[6] European Commission, 2022. Communication to the Commission. European Commission digital strategy- Next generation digital Commission C(2022) 4388 final. Brussels, 30.6.2022. https://commission.europa.eu/system/files/2022-06/c_2022_4388_1_en_act.pdf.

[7] AMI2030, 2022. Materials 2030 Roadmap. Advanced Materials Initiative 2030. December 2022. ⟨https://www.ami2030.eu/wp-content/uploads/2022/12/2022-12-09_Materials_2030_RoadMap_VF4.pdf⟩.

[8] European Commission, Internal Market, Industry, Entrepreneurship and SMEs, 2023. ⟨https://single-market-economy.ec.europa.eu/sectors/construction_en⟩ (accessed on 15 October 2023).

[9] European Commission, 2020. COM (2020) 98 Final. Communication from the Commission to the European Parliament, the Council, the European Economic and Social Committee and the Committee of the Regions: A new Circular Economy Action Plan for a Cleaner and more Competitive Europe. Brussels, 11/03/2020. https://eur-lex.europa.eu/resource.html?uri=cellar:9903b325-6388-11ea-b735-01aa75ed71a1.0017.02/DOC_1&format=PDF.

[10] K. Tibrewal, C. Venkataraman, H. Phuleria, et al., Reconciliation of energy use disparities in brick production in India, Nat. Sustain. 6 (2023) 1248–1257, https://doi.org/10.1038/s41893-023-01165-x.

[11] Davidovits, J., 1982. Mineral Polymers and Methods of Making Them, p. 6. United States; Patent no. 4.349.386, 1982.

[12] Davidovits, J., 2008. Geopolymer: Chemistry and Applications. June 2008, second ed. ISBN-13: 978-2951482012.

[13] M. Fawer, M. Concannon, W. Rieber, Life cycle inventories for the production of sodium silicates, Int. J. Life Cycle Assess. 4 (4) (1999) 207–212.

[14] R. Vinai, M. Soutsos, Production of sodium silicate powder from waste glass cullet for alkali activation of alternative binders, Cem. Concr. Res. 116 (2019) 45–56, https://doi.org/10.1016/j.cemconres.2018.11.008.

[15] P. Rożek, M. Król, W. Mozgawa, Geopolymer-zeolite composites: A review, J. Clean. Prod. 230 (2019) 557–579, https://doi.org/10.1016/j.jclepro.2019.05.152.

[16] N. Poumaye, O. Allahdin, G. Tricot, B. Revel, G. Billon, P. Recourt, M. Wartel, A. Boughriet, MAS NMR investigations on a metakaolinite-rich brick after zeolitization by alkaline treatments, ISSN 1387-1811, Microporous Mesoporous Mater. 277 (2019) 1–9, https://doi.org/10.1016/j.micromeso.2018.10.007.

[17] O. Allahdin, N. Poumaye, M. Wartel, A. Boughriet, Removal of (Natural and Radioactive) Cobalt by Synthetic Zeolites from Brick: Adsorption Isotherm, Mechanism, and Performance (in Batch and Column), Int. J. Sci. Res. Methodol. 19 (2) (2021) 41–70.

[18] ASTM D4318-10e1, Standard Test Methods for Liquid Limit, Plastic Limit, and Plasticity Index of Soils. Annual Book of ASTM Standards, ASTM International, West Conshohocken, PA, 2017.

[19] J.M. Moreno-Maroto, B. González-Corrochano, J. Alonso-Azcárate, L. Rodríguez, A. Acosta, Development of lightweight aggregates from stone cutting sludge, plastic wastes and sepiolite rejections for agricultural and environmental purposes, J. Environ. Manag. 200 (2017) 229–242, https://doi.org/10.1016/j.jenvman.2017.05.085.

[20] S. Yashima, Y. Kanda, S. Sano, Relationship between particle size and fracture energy or impact velocity required to fracture as estimated from single particle crushing. Powder Technol. 51 (1987) 277–282, https://doi.org/10.1016/0032-5910(87)80030-X.

[21] Y. Li, D. Wu, J. Zhang, L. Chang, Z. Fang, Y. Shi, Measurement and statistics of single pellet mechanical strength of differently shaped catalysts, Powder Technol. 113 (1-2) (2000) 176–184, https://doi.org/10.1016/S0032-5910(00)00231-X.

[22] J.M. Moreno-Maroto, B. González-Corrochano, J. Alonso-Azcárate, C. Martínez García, A study on the valorization of a metallic ore mining tailing and its combination with polymeric wastes for lightweight aggregates production, J. Clean. Prod. 212 (2019) 997–1007, https://doi.org/10.1016/j.jclepro.2018.12.057.

[23] EN 1097-6, 2013. Tests for mechanical and physical properties of aggregates - Part 6: Determination of particle density and water absorption. European Committee for Standardization.

[24] D.L. Bish, J.E. Post, Quantitative mineralogical analysis using the Rietveld full pattern fitting method, Am. Mineral. 78 (1993) 932–940.

[25] A.G. De la Torre, S. Bruque, M.A.G. Aranda, Rietveld quantitative amorphous content analyses. J. Appl. Crystallogr. 34 (2) (2001) 196–202, https://doi.org/10.1107/S0021889801002485.

[26] B.B. Jindal, T. Alomayri, A. Hasan, C.R. Kace, Geopolymer concrete with metakaolin for sustainability: a comprehensive review on raw material's properties, synthesis, performance, and potential application, Environ. Sci. Pollut. Res. 30 (2023) 25299–25324, https://doi.org/10.1007/s11356-021-17849-w.

[27] R.G. Milkey, Infrared spectra of some tectosilicates, Am. Mineral. 45 (9-10) (1960) 990–1007.

[28] J. Madejova, M. Janek, P. Komadel, H.J. Herbert, H.C. Moog, FTIR analyses of water in MX-80 bentonite compacted from high salinary salt solution systems, Appl. Clay Sci. 20 (2002) 255–271, https://doi.org/10.1016/S0169-1317(01)00067-9.

[29] I.K. Ilia, M.G. Stamatakis, T.S. Perraki, Mineralogy and technical properties of clayey diatomites from north and central Greece, Open Geosci. 1 (4) (2009) 393–403, https://doi.org/10.2478/v10085-009-0034-3.

[30] J.M. Moreno-Maroto, P. Delgado-Plana, R. Cabezas-Rodríguez, R. Mejía de Gutiérrez, D. Eliche-Quesada, L. Pérez-Villarejo, R.J. Galán-Arboledas, S. Bueno, Alkaline activation of high-crystalline low-Al_2O_3 Construction and Demolition Wastes to obtain geopolymers, J. Clean. Prod. 330 (2022) 129770, https://doi.org/10.1016/j.jclepro.2021.129770.

[31] EN 13055-1, 2002. Lightweight aggregates. Part 1: Lightweight aggregates for concrete, mortar and grout, European Committee for Standardization.

[32] B. Thakur, J. Singh, J. Singh, D. Angmo, A. Pal Vig, Biodegradation of different types of microplastics: Molecular mechanism and degradation efficiency, Sci. Total Environ. 877 (2023) 162912, https://doi.org/10.1016/j.scitotenv.2023.162912.

[33] I. El Bojaddayni, M.E. Küçük, Y. El Ouardi, I. Jilal, S. El Barkany, K. Moradi, E. Repo, K. Laatikainen, A. Ouammou, A review on synthesis of zeolites from natural clay resources and waste ash: Recent approaches and progress, Miner. Eng. 198 (2023) 108086, https://doi.org/10.1016/j.mineng.2023.108086.